The unique bond length to the axial ligand (Table IV) is significantly longer than the 2.087 (3) Å found[3a] for $[Fe(TPP)(TMSO)_2]^+$ or the 2.095 (2) Å value found[3b] for $[Fe(TPP)(H_2O)_2]^+$, both of which are high-spin species, but shorter than the 2.187 (11) Å value found[10] for the admixed intermediate-spin complex $[Fe(OEP)(THF)_2]^+$.

Averaged values of bond distances and angles in the porphinato core are given in Table IV; no unusual values are noted. Individual values of distances and angles are available as supplementary material. The hydroxylic hydrogen atom of the axial ethanol ligands are hydrogen bonded to the anion in both complexes. In $[Fe(TPP)(EtOH)_2]BF_4$, the oxygen to fluoride distance is either 2.68 or 2.79 Å at 99 K. These values are in good agreement with the O···F of 2.702 and 2.753 Å found in the structure of $[(CH_3OH)_2H]BF_4$ at −50 °C.[12] The corresponding O···O distances in $[Fe(TPP)(EtOH)_2]ClO_4$ are significantly longer at either 2.80 or 3.02 Å at 292 K. In both salts, the hydrogen bond distance depends on which anion orientation is closest to the ethanol oxygen atom, but all ethanol ligands are hydrogen bonded to an anion. This hydrogen bond network leads to a linear chain of alternating cations and anions in the crystal lattice.

Discussion

Crystalline $[Fe(TPP)(EtOH)_2]ClO_4$ is found not only to be isomorphous with $[Fe(TPP)(EtOH)_2]BF_4$ but also to show very similar structural features. A particularly interesting and unexpected feature is the rhombicity in the $Fe-N_p$ bond lengths. This rhombicity is seen in both the room- and low-temperature crystal structures of $[Fe(TPP)(EtOH)_2]BF_4$ and in the room-temperature crystal structure of $[Fe(TPP)(EtOH)_2]ClO_4$. The axial Fe–O bond lengths in the two complexes are also similar. These observations do not allow for an explanation of the differing temperature-dependent effective magnetic moments of $[Fe(TPP)(EtOH)_2]ClO_4$ and $[Fe(TPP)(EtOH)_2]BF_4$ on an obvious structural basis at the coordination group level.

We believe that the presence or absence of ferromagnetic ordering in the two salts arise from subtle differences in the hydrogen bonding between the ethanol ligands and the anion. With identical O–H donors and quite similar O and F acceptors, the lengths of the O–H–O and O–H–F hydrogen bonds are expected to be the same.[13] However, as noted in the Results, the O–H–O hydrogen bond lengths in the perchlorate salt are significantly longer than the O–H–F lengths in the tetrafluoroborate salt, and hence hydrogen bonding is slightly stronger in the latter. Previous evidence for the ready change of magnetic properties of the bis(aquo)iron(III) or the bis(ethanol)iron(III) system may be found from the reports of Scheidt and Reed,[2,14] Mitra et al.,[15] and Dolphin et al.[16] Mitra et al. report a $[Fe(TPP)(EtOH)_2]^+$ complex with a magnetic moment substantially reduced from that expected for a high-spin complex, while Dolphin reports a $[Fe(OEP)(EtOH)_2]^+$ complex with a very large Mössbauer quadrupole doublet. Unfortunately, neither bis(ethanol)iron(III) system has been characterized sufficiently to allow us to comment on any structural basis for their apparent differing magnetic properties. In the present case, however, it appears that the two salts have similar spin ground states but that they differ in their bulk magnetic properties because of small differences in the hydrogen bonding between ligand and anion.

Acknowledgment. We thank the National Institutes of Health (Grant GM-38401 to W.R.S.) and the Centre National de la Recherche Scientifique (URA 1194) for support of this research. We thank Jean-François Jacquot for his help with the SQUID measurements.

Supplementary Material Available: Figure S1, an ORTEP plot illustrating the disorder in the carbon positions of the axial ethanol ligands in $[Fe(TPP)(EtOH)_2]ClO_4$, Tables SI, SII, SV, and SVI, giving anisotropic thermal parameters, fixed hydrogen atom positions, bond distances, and angles for $[Fe(TPP)(EtOH)_2]ClO_4$, Tables SIII, SIV, SVII, and SVIII, giving anisotropic thermal parameters, fixed hydrogen atom positions, bond distances, and bond angles for $[Fe(TPP)(EtOH)_2]BF_4$, and Table SIX, giving complete crystallographic details (10 pages); listings of observed and calculated structure amplitudes (×10) (28 pages). Ordering information is given on any current masthead page.

---

(12) Mootz, D.; Steffen, M. *Angew. Chem., Int. Ed. Engl.* **1981**, *20*, 196.

(13) Ibers, J. A.; Hamilton, W. C. *Hydrogen Bonding in Solids*; W. A. Benjamin; New York, NY, 1968; Table 1-1.

(14) Reed, C. A.; Mashiko, T.; Bentley, S. P.; Kastner, M. E.; Scheidt, W. R.; Spartalian, K.; Lang, G. *J. Am. Chem. Soc.* **1979**, *101*, 2948.

(15) Mitra, S.; Date, S. K.; Nipankar, S. V.; Birdy, R.; Girerd, J.-J. *Proc.—Indian Acad. Sci.* **1980**, *89*, 511.

(16) Dolphin, D. H.; Sams, J. R.; Tsin, T. B. *Inorg. Chem.* **1978**, *17*, 711.

Contribution from the Department of Chemistry,
P.O. Box 3055, University of Victoria,
Victoria, BC, Canada V8W 3P6

Evidence for Ligand Isomerism in the Palladium(II) Complex of 1,4,7-Trithiacyclodecane

S. Chandrasekhar and A. McAuley*

Received July 13, 1991

Interest in homoleptic transition-metal complexes containing crown thioether ligands has seen significant increase only in the past five years.[1-15] Like the triaza macrocyclic analogues, trithia systems such as $[9]\text{-aneS}_3$ (**1**) provide examples of complexes where less common higher and lower oxidation states have been identified. Particular attention has been paid to weak interactions in axial sites of d^8 ions.[16] In the case of palladium(II), comment has been made[6,7,17] on the $[S_4 + S_2]$ configuration where four

---

(1) Setzer, W. N.; Ogle, C. A.; Wilson, G. S.; Glass, R. S. *Inorg. Chem.* **1983**, *22*, 266.

(2) Wieghardt, K.; Küppers, H. J.; Weiss, H. Z. *Inorg. Chem.* **1985**, *24*, 3067.

(3) Rawle, S. C.; Sewell, T. J.; Cooper, S. R. *Inorg. Chem.* **1987**, *26*, 3769.

(4) Bell, M. N.; Blake, A. J.; Gould, R. O.; Holder, A. J.; Hyde, T. I.; Lavery, A. J.; Reid, G.; Schröder, M. *J. Incl. Phenom.* **1987**, *5*, 169. Blake, A. J.; Gould, R. O.; Lavery, A. J.; Schroder, M. *Angew. Chem., Int. Ed. Engl.* **1986**, *25*, 274.

(5) Rawle, S. C.; Yagbasan, R.; Prout, K.; Cooper, S. R. *J. Am. Chem. Soc.* **1987**, *109*, 6181.

(6) Wieghardt, K.; Küppers, H. J.; Raabe, E.; Krüger, C. *Angew. Chem., Int. Ed. Engl.* **1986**, *25*, 1101.

(7) Blake, A. J.; Holder, A. J.; Hyde, T. I.; Roberts, Y. V.; Lavery, A. J.; Schröder, M. *J. Organomet. Chem.* **1987**, *323*, 261.

(8) Blower, P. J.; Clarkson, J. A.; Rawle, S. C.; Hartman, J. R.; Wolf, R. E., Jr.; Yagbasan, R.; Bott, S. G.; Cooper, S. R. *Inorg. Chem.* **1989**, *28*, 4040.

(9) Blake, A. J.; Gould, R. O.; Holder, A. J.; Hyde, T. I.; Lavery, A. J.; Odulate, M. O.; Schröder, M. *J. Chem. Soc., Chem. Commun.* **1987**, 118.

(10) Corfield, P. W. R.; Ceccarelli, C.; Glick, M. D.; Moy, I. W. Y.; Ochrymowycz, L. A.; Rorabacher, D. B. *J. Am. Chem. Soc.* **1985**, *107*, 2399.

(11) Rawle, S. C.; Cooper, S. R. *J. Chem. Soc., Chem. Commun.* **1987**, 308.

(12) Blake, A. J.; Gould, R. O.; Holder, A. J.; Hyde, T. I.; Schröder, M. *J. Chem. Soc., Dalton Trans.* **1988**, 1861.

(13) Blake, A. J.; Holder, A. J.; Hyde, T. I.; Schröder, M. *J. Chem. Soc., Chem. Commun.* **1989**, 1433.

(14) de Groot, B.; Loeb, S. H. *Inorg. Chem.* **1990**, *29*, 4084.

(15) Cooper, S. R. *Acc. Chem. Res.* **1989**, *21*, 141.

(16) Blake, A. J.; Holder, A. J.; Hyde, T. I.; Schröder, M. *J. Chem. Soc., Chem. Commun.* **1987**, 987.

(17) Grant, G. J.; Sanders, K. A.; Setzer, W. N.; VanDerveer, D. G. *Inorg. Chem.* **1991**, *30*, 4053. Sanders, K. A.; Grant, G. J.; Setzer, W. N. Re(III) and Pd(II) Complexes of Crown Thioethers. 201st National Meeting of the American Chemical Society, Atlanta, GA, 1991; Paper INOR 138.

0020-1669/92/1331-2663$03.00/0

Table I. Experimental Crystallographic Data for $[Pd([10]\text{-}aneS_3)_2](PF_6)_2\cdot 2CH_3CN$

formula	$PdC_{18}H_{34}S_6P_2F_{12}$	V	799.42 Å^3
MW	867.2	Z	1 molec/cell
space group	$P\bar{1}$ (No. 2)	T	22 ± 2 °C
cell params	a = 10.021 (3) Å	D_{calcd}	1.801 g/cm^3
	b = 10.800 (2) Å	D_{meas}	1.815 g/cm^3
	c = 8.043 (2) Å	λ (Mo Kα radiation)	0.71069 Å
	α = 111.57 (3)°	μ	12.52 cm^{-1}
	β = 95.40 (2)°	R^a	0.0517
	γ = 81.28 (2)°	$R_w{}^b$	0.0582

[a] $R = \sum||F_o| - |F_c||/\sum|F_o|$. [b] $R_w = [\sum w(|F_o| - |F_c|)^2/\sum w(|F_o|)^2]^{1/2}$; $w = 0.24/(\sigma^2 F + 0.001F^2)$.

planar sulfur donors are linked more closely to the metal ion than two axial donors at slightly greater remove. The proximity of such axial donors in an "entatic state" results in the relatively ready oxidation to the d^7, hexacoordinate complexes.[9,16]

In the present study, following the preparation of 1,4,7-trithiacyclodecane (**2**), an isomer (A) of $Pd([10]\text{-}aneS_3)_2{}^{2+}$ has been synthesized and characterized spectroscopically and structurally.[18] Oxidation produced the corresponding $[Pd(\mathbf{2})_2]^{3+}$ ion, which was characterized and by EPR spectroscopy. Comparisons are made with the corresponding nine-membered ring complexes and related complexes, especially with respect to the planar and axial interactions. Evidence is also found for reduction to a Pd(I) ion.

While this paper was being prepared for publication, a report[17] appeared on the preparation of the same species but with a different spatial arrangement of the ligands around the metal ion [isomer B]. Although both are trans isomers, they may be viewed as positional linkage isomers owing to the coordination of specific sulfur donors within the ten-membered ring. The contrasting species were derived from different solvent systems and crystallize in different space groups. Also noteworthy in the present investigation is the identification of strong secondary interactions with the acetonitrile solvent, as demonstrated by low-temperature (<−30 °C) ^{13}C NMR spectra.

Experimental Section

All chemicals were of reagent grade except where otherwise indicated. IR spectra were recorded on a Perkin-Elmer 283 grating spectrometer. High-field ^1H NMR and ^{13}C NMR spectra were measured with a Bruker WM250 or a Varian XL300 instrument. Electronic spectra were recorded on a Cary-5 spectrophotometer. EPR spectra were obtained with a Varian E6S spectrometer. Diphenylpicrylhydrazyl radical (dpph) was used as a field marker (g = 2.0037). Mass spectra were obtained from a Finnegan 330GC-MS instrument by electron impact and chemical ionization. Elemental analyses were performed by Microanalytical Services, Vancouver, BC, Canada. Electrochemical measurements were recorded with a Princeton Applied Research Model 273 potentiostat/galvanostat interfaced with an IBM/PC. Acetonitrile, freshly distilled from CaH_2/CH_3CN, was used with NEt_4BF_4 (0.1 M) as the supporting electrolyte. All potentials are reported against the Fc^+/Fc standard couple ($E_{1/2}$ of Fc^+/Fc vs NHE = 0.40 V) and were found to be internally consistent.

Synthesis of 1,4,7-Trithiacyclodecane ([10]-aneS$_3$, 2). Cyclization between 2-mercaptoethyl sulfide and 1,3-dibromopropane was carried out in dmf containing Cs_2CO_3 according to the methods of Buter and Kellogg.[19] Full details are presented elsewhere.[20] A similar procedure has been presented recently.[21] Colorless needle-shaped crystals of the product were obtained. Mp: 25 °C. m/e (EI): 194. m/e (CI): 195 (M + 1), 223 (M + 29), 235 (M + 41). ^1H NMR ($CDCl_3$): δ 1.61 (p, 2 H), 2.70 (m, 4 H), 2.89 (m, 8 H). ^{13}C NMR ($CDCl_3$): 4-line spectrum, δ 27.5 (1 C, $-C-CH_2-C$), 29.3 (2 C, $-CH_2-C-CH_2$), and two slightly magnetically inequivalent peaks at δ 33.2 and 33.5 (4 C, $-S-CH_2-CH_2-S-$).

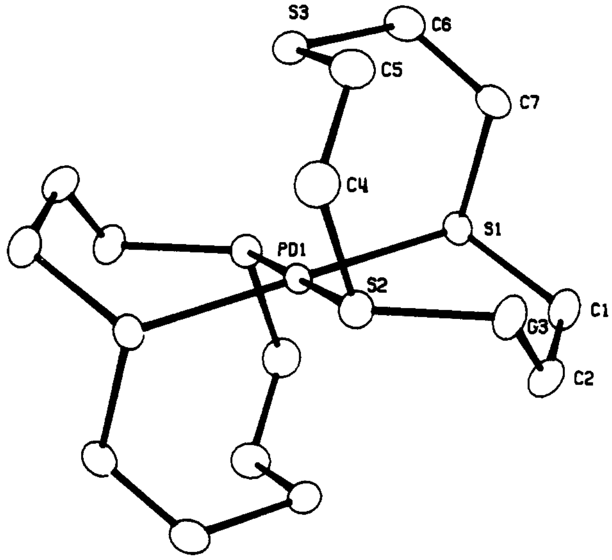

Figure 1. ORTEP diagram of the complex cation $[Pd([10]\text{-}aneS_3)_2]^{2+}$ with atomic labeling drawn with 25% thermal ellipsoids.

Table II. Fractional Atomic Coordinates and Temperature Parameters[a]

atom	x/a	y/b	z/c	U_{eq}, Å^2
Pd(1)	O (0)	0 (0)	0 (0)	299 (2)
S(1)	−9023 (13)	16839 (13)	−10941 (18)	366 (5)
S(2)	−3331 (15)	12650 (14)	30091 (18)	395 (5)
S(3)	−29565 (15)	−2751 (15)	1048 (21)	435 (6)
P(1)	30937 (20)	30159 (20)	66070 (25)	564 (8)
F(1)	4555 (7)	2906 (1)	6289 (20)	214 (8)
F(2)	2819 (10)	2010 (10)	4749 (11)	181 (5)
F(3)	1569 (8)	3183 (13)	6957 (14)	189 (7)
F(4)	3277 (17)	4151 (14)	8428 (12)	251 (9)
F(5)	2731 (14)	4208 (10)	5967 (15)	219 (8)
F(6)	3366 (17)	1996 (15)	7428 (23)	297 (12)
C(1)	−359 (7)	3288 (6)	326 (9)	52 (3)
C(2)	212 (7)	3400 (6)	2213 (9)	50 (2)
C(3)	−682 (7)	3056 (6)	3363 (8)	48 (2)
C(4)	−1856 (7)	831 (7)	3594 (8)	51 (3)
C(5)	−3145 (6)	877 (7)	2384 (9)	51 (3)
C(6)	−3426 (6)	790 (7)	−1225 (10)	54 (3)
C(7)	−2729 (6)	2027 (7)	−701 (9)	48 (3)
C(8)	4315 (8)	3944 (8)	2254 (11)	69 (3)
C(9)	3225 (8)	5094 (7)	2679 (10)	56 (3)
N(1)	2396 (8)	5943 (8)	2988 (10)	80 (3)

[a] Estimated standard deviations are given in parentheses. Coordinates × 10^n, where n = 5, 5, 4, 4, and 4 for S, P, F, C, and N. Temperature parameters × 10^n, where n = 4, 4, 4, 3, 3, and 3 for Pd, S, P, F, C, and N. U_{eq} = the equivalent isotropic temperature parameter. $U_{eq} = {}^1/_3\sum_i\sum_j U_{ij}a_i{}^*a_j{}^*(a_i a_j)$. Primed values indicate that U_{iso} is given. $T = \exp[-(8\pi^2 U_{iso}(\sin^2\theta)/\lambda^2)]$.

$[Pd([10]\text{-}aneS_3)_2](PF_6)_2$: Isomer A. A suspension of the ligand, **2**, 0.125 g (1.1 mmol) in 20 mL of H_2O/MeOH (1/1 v/v), was stirred for 15 min at 45 °C. To this, a solution of K_2PdCl_4, 0.167 g (0.51 mmol) in H_2O/CH_3OH (1/1 v/v, 20 mL), was added dropwise. The green solution formed was stirred at room temperature for 30 min and filtered. Following reduction of the filtrate to a small volume, addition of NH_4PF_6 yielded a green solid, which was recrystallized by diffusion of ether into CH_3CN solutions. The resultant blue crystals of the complex $[Pd([10]\text{-}aneS_3)_2](PF_6)_2\cdot 2CH_3CN$ were filtered out and dried under vacuum. Yield: 244 mg; 61%. Anal. Calcd for the green solid, $C_{14}H_{28}S_6PdP_2F_{12}$: C, 21.41; H, 3.59. Found: C, 21.47; H, 3.59. The UV-visible spectrum of the $[Pd([10]\text{-}ane\text{-}S_3)_2]^{2+}$ ion shows one broad peak at 598 nm (ϵ = 84 M^{-1} cm^{-1}) assigned to a d–d transition and three charge-transfer bands at 314 nm (ϵ = 10800 M^{-1} cm^{-1}), 277 nm (ϵ = 11300 M^{-1} cm^{-1}), and 209 nm (ϵ = 8000 M^{-1} cm^{-1}). No other absorption bands were observed. These values are close to those reported recently.[17]

Crystal Structure of $[Pd([10]\text{-}aneS_3)_2](PF_6)_2\cdot 2CH_3CN$. Pertinent crystallographic data are given in Table I and in the supplementary material provided. The molecule has an inversion center at the Pd atom. Thus, the asymmetric unit consists of half a molecule of the complex cation, one $PF_6{}^-$ anion, and one molecule of CH_3CN as solvent of crystallization. The refinement converged to an R value of 0.0517 and R_w = 0.0582, with a maximum shift/esd of 0.043 in the final cycle. A final difference map had a maximum peak of 0.895 e Å^{-3}.

---

(18) Chandrasekhar, S.; McAuley, A. Synthesis and Solid-state Crystal structure of $[Pd([10]aneS_3)_2]^{2+}$ Ion. 72nd Canadian Chemical Conference and Exhibition, Victoria, BC, Canada, June, 1989; Paper INOR 815.

(19) Buter, J.; Kellogg, R. M. *J. Org. Chem.* **1981**, *46*, 4481; *Org. Synth.* **1987**, *65*, 150.

(20) Chandrasekhar, S. Ph.D. Dissertation, University of Victoria, Victoria, BC, Canada, 1991.

(21) Grant, G. J.; Carpenter, J. P.; Setzer, W. N.; Van Derveer, D. G. *Inorg. Chem.* **1989**, *27*, 4128.

Table III. Selected Interatomic Distances (Å) and Bond Angles (deg)[a]

S(1)-Pd	2.330 (1)	S(2)-Pd-S(1)	96.6 (0)
S(2)-Pd	2.328 (1)	S(3)-Pd-S(1)	82.7 (0)
S(3)···Pd	3.034 (1)	S(3)-Pd-S(2)	81.1 (0)

[a] Estimated standard deviations are given in parentheses.

Results and Discussion

The ion is square-planar (Figure 1) but shows significant axial interactions with the endodentate noncoordinated sulfur atoms. Fractional atomic coordinates and bond lengths and bond angles are given in Tables II and III. The mean Pd-S equatorial bond length is 2.329 (1) Å, longer than that found for the other isomer identified (2.27 Å)[17] but comparable with the $Pd(S_3)^{2+}$,[6,7] $Pd(18S_6)^{2+}$,[4,22] and other N_2S_4 ligand systems.[23] The axial sulfur atoms are located at 3.034 (1) Å from the metal center, considerably shorter than in isomer B (3.11 Å). The reason for the differences is provided in analysis of the spatial arrangements of the ligands. In isomer A, the sulfur atoms of the six-membered chelate ring are in the plane, while in isomer B it is the S donors of five-membered rings that are bonding. The bond distances reflect the increased binding strengths of the five-membered rings vis-a-vis the six in the boat configuration.

The equatorial bond angle S(1)-Pd-S(2) of 96.6 (0)° is larger than that in isomer B (88.8°) and also the corresponding $Pd([9]\text{-ane}S_3)^{2+}$ ion (88.63 (11)°) owing to the location of the six-membered chelate ring in the present complex. The presence of the five-membered "chelate" rings subtending the axial sites reduces the flexibility of the apical sulfur in its ability to be located in a position for coordination. This may be seen as resulting in a 12.2° angle between the normal to the PdS_4 plane and the Pd-S(3) vector, the value being somewhat larger than that in isomer B (9.9°) and $[Pd([9]\text{-ane}S_3)_2]^{2+}$ (7.80°).

Of interest is the cell packing for the complex (supplementary figure), where the Pd cations and the CH_3CN molecules lie in alternating planes, while the PF_6^- anions lie in a perpendicular plane. The position of the acetonitrile is such that the N atom is directed toward the palladium through the center of the pseudotrigonal face of a chelating ligand. As such, the solvent nitrogen may approach the Pd atom to a distance of ~6 Å. This feature has implications when considering the low-temperature ^{13}C NMR spectra. In the ^{13}C NMR spectrum at ambient temperatures a seven-line peak centered at δ 1.3 is seen due to the methyl group of the CD_3CN solvent (supplementary figure). A feature at δ 118.6 is seen due to the C atom of the nitrile. As the temperature is lowered, the solvent peaks are broadened, yielding two well-defined septets centered around δ 1.3 at -40 °C. Also two lines at δ 118.5 and 118.7 are distinctly seen from the carbon of the nitrile group. A third peak observed at δ 118.9 becomes more pronounced as the temperature is lowered due to a third type of CD_3CN molecule. The associated septet is just discernible at lower δ. Observation of three distinctive sets of solvent resonances implies that the solvent is partitioned into three magnetic environments, the first and second solvation spheres and the bulk solvent.

The Pd(II) complex is readily oxidized by NO^+ in acetonitrile to a Pd(III) ion, which $g_{\parallel} = 2.005$ and $g_{\perp} = 2.042$, characteristic of a tetragonally elongated octahedral complex ion. In addition to the reversible oxidation, there is electrochemical evidence for the formation of a Pd(I) ion under reducing conditions.

These g values compare well with those obtained for $[Pd([9]\text{-ane}S_3)_2]^{3+}$ and $[Pd([9]\text{-ane}N_3)_2]^{3+}$.[7,24] The axial S atoms in $[Pd([10]\text{-ane}S_3)_2]^{2+}$ are suitably disposed to promote octahedral stereochemistry around the d^7 metal ion. The unpaired electron occupies the d_{z^2} orbital as has been seen in the EPR spectra of other Pd(III) species.

Acknowledgment. Support from the Natural Sciences and Engineering Research Council and the University of Victoria is gratefully acknowledged. Assistance of Ms. K. Beveridge in the X-ray structure determination is greatly appreciated. Assistance of Prof. S. O. Chan and Ms. L. Darge, Department of Chemistry, University of British Columbia, in the recording of the variable-temperature NMR spectra is also greatly appreciated. We thank Dr. T. W. Whitcombe for helpful discussions.

Supplementary Material Available: Table S1, listing experimental crystallographic data for the complex, Tables S2-S4, listing interatomic bond distances and angles, anisotropic temperature parameters, and selected intermolecular distances, Table S6, listing data on mean planes, and figures showing a diagram of the molecular packing, a ^1H NMR spectrum of the complex cation in CD_3NO_2, a ^{13}C NMR spectrum including the solvent region, and a representative ESR spectrum (17 pages); Table S5, listing calculated and observed structure factors (10 pages). Ordering information is given on any current masthead page.

---

[22] Reid, G.; Schröder, M. *Chem. Soc. Rev.* **1990**, *19*, 239.
[23] Blake, A. J.; Reid, G.; Schroder, M. *J. Chem. Soc., Dalton Trans.* **1990**, 3363.
[24] McAuley, A.; Whitcombe, T. W. *Inorg. Chem.* **1988**, *27*, 3090.

Contribution from the Department of Chemistry,
Texas Christian University, Fort Worth, Texas 76129

Synthesis and Solvolysis of Benzylamine-Boranes

Kevin E. Bell and Henry C. Kelly*

Received July 19, 1991

Introduction

The reactivity of donor base-borane addition compounds is highly sensitive to structural variations both in the donor portion of the molecule and in the coordination sphere of boron. Regarding amine-BH_3 adducts, it has been shown that solvolysis in water or mixed aqueous solvents occurs via two mechanisms, one presumed to involve rate-determining dissociative activation of the B-N bond (Scheme I) and the second involving electrophilic displacement of BH_3 through attack of the proton of a general acid at nitrogen (Scheme II).[1-8] Rates are sensitive to electronic and steric effects, and the nature of the amine largely determines whether the acid-independent or acid-dependent pathway will be dominant.[1] Substitution of one or more anionic ligands, e.g., halide, CN^-, and N_3^- for boron-bonded (hydridic) hydrogen, also has been shown to give rise to a change in hydrolysis mechanism with the reaction path dependent on the specific ligand.[9-12]

In this paper, we report the synthesis and hydrolytic reactivity of several substituted benzylamine-boranes and examine the influence of the intervening CH_2 group on effects of aryl substitution on reaction at the $\equiv N-BH_3$ site. Since the effectiveness of a donor-borane adduct as a hydridic reagent in aqueous media is dependent, in large measure, on the kinetic stability of the adduct toward hydrolytic decomposition, this study also has implications with respect to the utility of benzylamine-boranes as practical synthetic reagents.

Experimental Section

Materials. Amines, boron trifluoride-diethyl ether complex, tetrahydrofuran (THF), and *p*-dioxane were obtained from Aldrich. The $BF_3 \cdot Et_2O$ was distilled in vacuo prior to use. Sodium tetrahydridoborate was obtained from Aldrich or Morton International in 98% purity and dried in vacuo. The THF was boiled under reflux in a nitrogen atmosphere over CaH_2 for several hours and then collected by decantation and distilled from sodium and

---

(1) Kelly, H. C.; Marchelli, F. R.; Giusto, M. B. *Inorg. Chem.* **1964**, *3*, 431.
(2) Ryschkewitsch, G. E. *J. Am. Chem. Soc.* **1960**, *82*, 3290.
(3) Ryschkewitsch, G. E.; Birnbaum, E. R. *Inorg. Chem.* **1965**, *4*, 575.
(4) Kelly, H. C. *Inorg. Chem.* **1966**, *5*, 2173.
(5) Kelly, H. C.; Underwood, J. A., III. *Inorg. Chem.* **1969**, *8*, 1202.
(6) Kelly, H. C.; Marriott, V. B. *Inorg. Chem.* **1979**, *18*, 2875.
(7) Minter, D. E.; Kelly, C. R.; Kelly, H. C. *Inorg. Chem.* **1986**, *25*, 3291.
(8) (a) Kreevoy, M. M.; Hutchins, J. E. C. *J. Am. Chem. Soc.* **1972**, *94*, 6371. (b) Kreevoy, M. M.; Hutchins, J. E. C. *J. Am. Chem. Soc.* **1969**, *91*, 4329.
(9) Lowe, J. R.; Uppal, S. S.; Weidig, C.; Kelly, H. C. *Inorg. Chem.* **1970**, *9*, 1423.
(10) Weidig, C.; Lakovits, J. M.; Kelly, H. C. *Inorg. Chem.* **1973**, *15*, 1783.
(11) Weidig, C.; Uppal, S. S.; Kelly, H. C. *Inorg. Chem.* **1974**, *13*, 1763.
(12) Skillern, K. R.; Kelly, H. C. *Inorg. Chem.* **1977**, *16*, 3000.

0020-1669/92/1331-2665$03.00/0